Wavelet-frequency analysis for the detection of discontinuities in switched system models of human balance

Salam Nema[a,*], Piotr Kowalczyk[a], Ian Loram[b]

[a]*School of Computing, Mathematics and Digital Technology, Manchester Metropolitan University,Manchester, U.K.*
[b]*School of Healthcare Science, Manchester Metropolitan University, Manchester, U.K.*

Abstract

This paper is concerned with detecting the presence of switching behavior in experimentally obtained posturographic data sets by means of a novel algorithm that is based on a combination of wavelet analysis and Hilbert transform. As a test-bed for the algorithm, we first use a switched model of human balance control during quiet standing with known switching behavior in four distinct configurations. We obtain a time-frequency representation of a signal generated by our model system. We are then able to detect manifestations of discontinuities (switchings) in the signal as spiking behavior. The frequency of switchings, measured by means of our algorithm and detected in our models systems, agrees with the frequency of spiking behavior found in the experimentally obtained posturographic data.

Keywords: Switched systems, Wavelets, Normalized Hilbert transform, Discontinuities, Instantaneous frequency.

1. Introduction

Many engineering and biological systems are characterized by the presence of switchings and/or dynamics evolving over multiple time scales. For instance, brain activity, which is measured by means of Electroencephalography (EEG), is characterised by natural time scales related to spiking and bursting behaviour, with the dynamics evolving over time scales ranging from milliseconds to minutes. Feedback control mechanisms used, for instance, in power engineering contain switching elements which, on the macroscopic scale, may be considered as acting instantaneously. In robotics, the control problem of biped robots has several characteristics such as the inherent instability of two-legged motion, high-dimensional dynamics, and the existence of different phases of the walking cycle, which require a fuzzy switching control system to represent the continuous-time dynamics and discrete event dynamics of a walking biped (Liu et al., 2007).

In recent years, much of research effort has been spent on understanding the character of control strategy which ensures human balance control during quiet standing. Human balance control during

---

[*]Corresponding Author - E-mail: s.nema@mmu.ac.uk

quiet standing is often modelled using linear, continuous time systems (Jeka et al., 2004; Kiemel et al., 2002). These models exclude thresholds, instantaneous switchings and time variant processes such as open loops. However, impulsive like muscle movements have been detected during quiet standing (Bottaro et al., 2008), and so it should come as no surprise that among the biomechanics community switched and intermittent control models have been used to account for sway dynamics during quiet standing (Gawthorp et al., 2011). There is currently a controversy whether human quiet standing can be better captured by a linear time invariant process, or whether it is an intermittent or switched control that can better capture the balance control mechanism. The aim of the current work is to find in experimental posturographic data sets the possible existence of switching transitions (discontinuities). To this aim we propose an algorithm which would allow one to detect time instances of the occurrences of discontinuities in signals generated by switched systems with noise. In particular, we are interested in determining time instances when a PD (proportional-derivative) control is switched on/off when a state variable crosses some threshold value.

Several methods have been proposed in the literature for different applications to detect change points in the process data. For instance, auto-covariance methods (Killick and Eckley, 2013), time-domain methods (Thornhill and Horch, 2007; Theron and Aldrich, 2004) and spectral methods (Antoniadis and Gijbels, 2002; Babji et al., 2009) have been considered. In particular, Killick and Eckley (Killick and Eckley, 2013) introduced a method to detect changes in general auto-covariance structure within non-stationary time series data. Their method is based on locally stationary wavelet framework and does not assume a specific structure for the auto-covariance. Thornhill and Horch (Thornhill and Horch, 2007) developed a time-domain approach for detecting and diagnosing plant-wide control system disturbances in chemical processes. Antoniadis and Gijbels (Antoniadis and Gijbels, 2002) have contributed to the methodology available for dealing with the detection and the estimation of the location of discontinuities by implementing a curve fitting estimation method followed by wavelet smoothing to detect and locate discontinuities in a time series data. Babji et al. (Babji et al., 2009) proposed a method based on Hilbert-Huang Transform to detect control valve nonlinearity. The nonlinearity can be captured by Intrinsic Mode Functions obtained from the Empirical Mode Decomposition of the process output. Inoue and Sakaguchi (Inoue and Sakaguchi, 2015) proposed an analysis method for extracting intermittent discontinuities observed in human hand movement using the amplitude and phase information of the complex wavelet transform. It was found that the discontinuous changes in the velocity profile roughly corresponded to specific peak positions in the jerk profile, and confirmed that these peaks could be effectively detected by continuous wavelet transform with a Gaussian derivative kernel.

Each of these methods relies on the recognition of certain characteristics of the process data, and they are dependent on the domain of analysis. The character of discontinuities that we are concerned with here is different from all these cases in so far that we are interested in revealing

discontinuities in a deterministic signal buried in noise. Let us suppose that we are concerned with a switched system with additive noise that is switching between two distinct differentiable vector fields when a control variable crosses some threshold value . A system trajectory, ignoring the presence of noise, will contain discontinuity in one of its derivatives. Added noise will have some 'linearising' effect on this 'deterministic' discontinuity (Gammaitoni, 1995). The question now arises how could one detect these types of discontinuities in a signal. That is, to investigate the 'deterministic' part of a stochastic system it is required to separate the 'deterministic' components of a signal 'buried' in additive noise. Thus we need to reconstruct the signal without noise components.

As explained by Boashash in (Boashash, 1992), for non-stationary processes, produced signals do not lend themselves well to decomposition into sinusoidal components, and they cannot be represented in a meaningful way by Fourier expansions. Consequently, a time series data of a switched or time variant stochastic system cannot be represented by a Fourier series due to the apparent presence of non-stationarity. In such cases, the notion of frequency looses its effectiveness, and one needs to use a parameter which accounts for the time-varying nature of the process. Therefore, for non-stationary signals, in which frequency value changes at any moment, it is more useful to characterise the signal in terms of its Instantaneous Frequency (IF), which is a time dependent representation of the frequency of a signal at any moment. It is the instantaneous frequency which will provide us with the information on the presence of discontinuities in a signal at any given time instant.

In this article, we propose a novel Wavelet-Frequency Analysis algorithm for detecting discontinuities in time series data of switched systems with additive white noise by combining the advantages of discrete Wavelet decomposition technique and Normalized Hilbert Transform (NHT). The wavelet analysis can extract important information of switched model systems at different time intervals, and the computed instantaneous frequency can effectively provide us with the information on the presence of discontinuities in the signal at any given time instant. In the designed algorithm, we introduce an energy wavelet decomposition technique to resolve one key obstacle for computing a meaningful instantaneous frequency from a multicomponent signal by reducing it to a collection of monocomponent functions. Once we obtain the monocomponent signals, the instantaneous frequency can be computed using the normalized Hilbert transform method. Therefore, a practical wavelet filtering technique has been used to help to decompose the data into monocomponents. It was found that, this decomposition approach has effectively worked as a special band pass filter. One of the advantages of this technique is that it allows us to decompose the data into a set of independent coefficients with a coefficient corresponding to each of the orthogonal basis functions. These monocomponents were then analyzed and recombined into a signal that contained the instantaneous frequency reflections, but not the switched system main response or the noise.

The paper is organized as follows: Sec. 2.1 discusses the wavelet-based method that we are going

to use, whereas Sec. 2.2 presents an outline of the frequency analysis technique for estimating the instantaneous frequencies. Sec. 2.3 illustrates the details of the proposed algorithm. Then in Sec. 3, we present the detection of discontinuous nonlinearities in simulated data sets produced by different model systems. We also consider posturographic data sets in which we identify spiking features resembling those found in our switched model systems. At the end of this section, we evaluate the performance of our algorithm by comparing it against other detection methods available in the literature. Finally, Sec. 4 concludes the paper and outlines our future work.

2. Algorithm Framework

2.1. Wavelet Analysis

2.1.1. Wavelet transformation of signals

Wavelet transform is being used in many real-time signal and image processing applications due to its efficiency in multi-resolution analysis (Liu et al., 2008). Wavelet transformation maps data from the time domain to the wavelet domain, and the result is a vector of the same size. The wavelet transform decomposes a function into a weighted sum of its various frequency components. The time and frequency localization of wavelets makes it into a powerful tool for feature detection. Wavelet transformation is linear and it can be defined by matrices of dimensions $m \times m$ if it is applied to inputs of size m. The signal $f(t)$ is examined by the wavelet transform with the help of a mother wavelet, say ψ. Thus, the wavelet transform is given by

$$F_\omega(a, b) = \frac{1}{\sqrt{a}} \int_{-\infty}^{\infty} f(t) \psi \left(\frac{t - b}{a} \right) dt \tag{1}$$

The last equation shows how a function $f(t)$ is decomposed into a set of basis functions $F_\omega(a, b)$. The variables a and b, scale and shift, are the new dimensions after the wavelet transform. The parameter b shifts the wavelet so that local information about f, at time $t = b$, is contained in $F_\omega(a, b)$, and the parameter a controls the frequency value of the wavelet for a particular shift b.

It is useful to decompose the data into wavelet coefficients using stationary discrete wavelet transform because most of the coefficients will be close to zero, with only a few coefficients carrying most of information. Consequently, the original signal $f(t)$ can be reconstructed in a way that depends on the aim of the analysis. Successful reconstruction also depends on the original choice of ψ. If the wavelet ψ is such that

$$C_\psi = 2\pi \int_{-\infty}^{\infty} \frac{|\hat{\psi}(\omega)|^2}{|\omega|} d\omega \tag{2}$$

where $\hat{\psi}$ denotes the Fourier transform of ψ, the original signal $f(t)$ can be reconstructed as

$$f(t) = \frac{1}{C_\psi} \int_{-\infty}^{\infty} \int_{-\infty}^{\infty} |a|^{-1/2} \psi \left(\frac{t - b}{a} \right) F_\omega(a, b) \frac{da\,db}{a^2} \tag{3}$$

4

One of the advantages of wavelet transformation is that it allows the use of long time intervals when we want more precise low frequency information, and shorter intervals where we want high frequency information. It should be noted that, in order to isolate signal discontinuities, it is more efficient to use a very short basis function. Hence, the proposed method performs a multilevel stationary wavelet decomposition using a specific biorthogonal wavelet called Daubechies. This wavelet family constructs compactly supported orthogonal wavelets with a preassigned degree of smoothness. These wavelet bases are defined as a pair of mutually orthogonal bases neither of which is an orthogonal basis. The detailed properties of this wavelet can be found in Daubechies' monograph (Daubechies, 1992).

2.1.2. Wavelet decomposition tree

The designed algorithm performs the wavelet decomposition of the time series data based on the theory of orthogonal filter banks described in (Strang and Nguyen, 1997). In this approach, pyramid or cascade procedures process the data at different scales, ranging from fine to coarse, in a tree-like algorithm, in such a way that the signal can be decomposed to different levels, then de-noised, enhanced or compressed by appropriate scale-wise treatment. Such idea gives a constructive and efficient recipe for performing the discrete wavelet transformation. It links the wavelet coefficients from different levels in the transformation using parallel filtering.

At level (i), the wavelet decomposition process starts by splitting a given time series data into two parts by using a two-channel filter bank in combination with down-sampling by a factor of 2. After splitting, we obtain a vector of approximation coefficients A_{i+1} and a vector of details coefficients D_{i+1}, both at different scales. Then the next step consists of splitting the new approximation coefficient vector A_{i+1} into two parts to obtain a new approximation vector A_{i+2} and details vector D_{i+2}. This process continues till we build the wavelet decomposition tree with a number of approximation and details vectors A_{i+n} and D_{i+n}, respectively, where n is the number of decomposition levels. Note that, at each stage of the filtering process, the approximation vector is obtained by using a low pass filter to extract the low frequency components while the details vector is obtained using a high pass filter to extract the high frequency components. Each details or approximation coefficients vector can be reconstructed at any decomposition level using the same filtering approach combined with up-sampling by a factor of 2.

2.2. Frequency analysis

2.2.1. Instantaneous frequency

The instantaneous frequency is a time dependent representation of the frequency of a signal at any moment(Boashash, 1992). It can be described by considering the following time-domain

procedure:

$$z(t) = s(t) + jH[s(t)] = a(t)e^{j\phi(t)} \tag{4}$$

where $z(t)$ is the analytic signal, $s(t)$ is the real signal and H is the Hilbert Transform defined as

$$H[s(t)] = p.v. \int_{-\infty}^{\infty} \frac{s(t-\tau)}{\pi\tau}d\tau \tag{5}$$

where $p.v.$ denotes the Cauchy principal value of integral (Marple, 1999).

By considering the problem of positioning a signal $s(t)$ in the frequency domain, we construct the analytic signal $z(t)$ as defined in (4). Its spectrum, $Z(f)$, is given by

$$Z(f) = \int_{-\infty}^{\infty} a(t)e^{j[\phi(t)-2\pi ft]}dt. \tag{6}$$

The application of the stationary phase principle indicates that this integral will have its largest value at the frequency f_s , for which the phase is stationary, such that

$$\frac{d}{dt}[\phi(t) - 2\pi f_s t] = 0. \tag{7}$$

Equation (7) leads to the definition of the instantaneous frequency as

$$f_s = \frac{1}{2\pi}\frac{d\phi(t)}{dt}. \tag{8}$$

This indicates that if f_s is a function of t, $f_s(t)$ provides a measure of the signal energy concentration as a function of time.

2.2.2. Normalized Hilbert transform method

The instantaneous frequency for any monocomponent data can be computed by applying Hilbert transform in equation (5) combined with a normalization scheme. This approach will enable us to get an exact instantaneous frequency (Huang et al., 2009). We first compute the absolute value of Hilbert transform of the signal $s(t)$ to produce an envelope to the data, then this envelope $e(t)$ is used as the base for normalizing the data as follows $n(t) = \frac{s(t)}{e(t)}$, where $n(t)$ is the normalized data. Ideally, $n(t)$ should have all the extrema with unity value. Such normalization is particularly important because it enables us to compute the phase angels directly without any approximation. The next step is to apply Hilbert transform to the normalized data to obtain an analytic complex signal $z(t)$ such that

$$z(t) = x(t) + jy(t) = a(t)e^{j\phi(t)} \tag{9}$$

where $a(t)$ is an absolute value of the signal and $\phi(t)$ is the phase function. The imaginary part includes phase information that depends on the phase of the original data. Once the phase angles are determined, the instantaneous frequency f_s can be computed as the derivative of the phase function $\phi(t)$ by using equation (8).

2.3. The proposed algorithm

In this section, we present a novel algorithm aimed at determining discontinuities in a signal buried in noise generated by switched control systems. The developed algorithm is mainly based on a combined frequency and wavelet analysis approach. We first present an outline guide to the algorithm steps as shown below:

1. Choose a wavelet ψ and a decomposition level n.

2. Compute the wavelet decomposition of a given time series data down to level n.

3. For each level, from 1 to n, determine the details wavelet coefficients.

4. Identify the highest energy components of the details coefficients using energy entropy based method.

5. Reconstruct and combine the identified details components.

6. Apply Hilbert transform to get an envelope to the identified data.

7. Normalize the monocomponents data using Hilbert's envelope.

8. Compute the phase angles of the identified monocomponents using NHT method.

9. Compute the instantaneous frequency as the derivative of the phase function to produce a time-frequency representation of the signal.

10. Identify the peaks in the time-frequency data representation, which would then correspond to abrupt changes in system dynamics.

In our case studies in Sec. 3, we start the algorithm by decomposing the time series data down to level seven. The selection of a suitable number of levels is based on the frequency of the data components. This process splits the data into different frequency bands from high to low frequencies. Level one to five contains highest frequencies, which mostly consist of noise, while levels eight and above contain the basic response of the system. All of these components are therefore discarded. The other levels are considered for further analysis. The chosen wavelet for this problem is Daubechies wavelet with six vanishing moments (*db*6). This wavelet is superior for representing polynomial behaviour in addition to its ability to detect the discontinuities. It has scaling ϕ and wavelet ψ functions both for the decomposition and reconstruction processes. The scaling function ϕ and its coefficients detects localized low frequency information, while the wavelet ψ and its coefficients detects localized high frequency information.

The wavelet coefficients are then obtained by applying the discrete wavelet transform. At each decomposition level, the output of the discrete wavelet transform brings out a high resolution data

(details coefficients) while at the same time smoothing the remaining data (approximation coefficients). The wavelet coefficients are placed in a transformation matrix and ordered using two patterns, one contains the smoothed data, and the other brings out the details information. This decomposition technique enables to detect more easily any change points by looking for details coefficients in modulus not at the full range of all the data levels.

We use an energy entropy based method for choosing the right decomposition level. Entropy measures the repeatability or predictability within a time series to quantify the complexity of a signal produced by a given system (Richman and Moorman, 2000).

In our approach, the energy E of each level at time k, and for scale j can be approximated by $E(j,k) = |s_i(t)|^2$, where $s_i(t)$ is the wavelet coefficients at level i. Summing this energy for all discrete times k and scales j leads to an approximation of the energy content at each level i as $E(i) = \sum\limits_{j} \sum\limits_{k} E(j,k)$. Then, we follow the Shannon entropy, which is a probability density function P_E defined as a ratio between the energy of each level and the total energy, that is $P_E(i) = \dfrac{E(i)}{\sum\limits_{i=1}^{n} E(i)}$.

This corresponds exactly to the probability density distribution of energy across the scales. Then, we calculate the value of energy entropy E_n for each decomposition level i, which computes the variation of the degrees of complexity of noise as:

$$E_n(i) = \sum_{i=1}^{n} -P_E(i) ln(P_E(i)). \tag{10}$$

The greater value of E_n reflects more randomness and signal complexity. The selection of the decomposition level to be analyzed was based on the difference of energy distribution between the noisy time series data at each level. The highest difference value is used to measure the degree of complexity of the data for all the levels. The highest difference value indicates a jump between the low and high level of noise. Hence, the value of entropy E_n at each level i is calculated. Then, the highest difference value of E_n between two consecutive levels is determined. The higher decomposition level is chosen for further analysis. The signal of the selected level should have lower degree of complexity and contains low noise influences. Consequently, it is found that the first few levels contain highest frequencies that mostly consist of noise, while higher levels contain the basic response of the system. All of these components therefore should be discarded and only the levels that carry most of the information of the signal have to be considered for further analysis.

Then, the algorithm passes the details coefficients vectors through the same filtering process to reconstruct these components. Note that, in order to reconstruct the details components through the filter banks process, we feed in a vector of zeros in place of the approximation coefficients vector. The next step of the algorithm process is to apply the Hilbert transform, described by equation (5), to produce an envelope to the monocomponents data. This envelope is used to normalize the data. This normalization allows us to compute the phase angles of the monocomponents directly

by using the NHT method. Then the instantaneous frequencies are calculated using equation (8). The strongest peaks, in the time-frequency representation, allow us to identify any abrupt changes in the time series data.

3. Numerical Experiment

In this section, we apply our algorithm to identify discontinuous nonlinearities in time series data produced by four switched model systems, which can be thought of as models of human balance control during quiet standing. All these different switched models are presented in order to verify how well does the algorithm perform. We apply our procedure to the time series data produced by the switched control systems to investigate the effect of additive white noise or time delay on detecting discontinuities. There is also a fifth case which presents the analysis of experimental posturographic time series data by means of our algorithm. At the end of this section, the performance of the algorithm is compared against other detection methods available in the literature.

3.1. Switched model of human balance control

We will model human neuromuscular control during quiet stance using an inverted pendulum model (Craik, 1947; Jeka et al., 2000; Winter et al., 2001). That is, we assume that the human body is represented as a single rigid link of some length with the centre of mass m located at the distance h above the ground. The only force acting on the mass is that of gravity, and we additionally assume that the neuromuscular control is applied to the system through a Proportional-Derivative (PD) control signal acting with a certain time delay τ (the delay is present due to neural processing). Moreover, there is a dead-zone present in our model system due to a finite accuracy of sensing. That is, the PD control is switched on when the position signal, $\theta(t - \tau)$, exceeds certain fixed, but non-zero, value θ_0. A noise torque is modelled using an additive Gaussian white noise, say $\zeta(t)$, of intensity σ. The sway motion will be modelled by a delay differential equation with additive noise as:

$$J\ddot{\theta} = mgh\sin(\theta) + \sigma\zeta(t) \quad \text{for} \quad |\theta(t - \tau)| \leq \theta_0, \tag{11}$$

when there is no control applied to the system, and

$$J\ddot{\theta} = mgh\sin(\theta) + T + \sigma\zeta(t) \quad \text{for} \quad |\theta(t - \tau)| > \theta_0. \tag{12}$$

when a PD controller is switched on; J is the moment of inertia of the body about the ankle joint axis. The delay terms are present in the applied torque generated by the PD controller. Namely

$$T = -K_p\theta(t - \Delta) - K_d\dot{\theta}(t - \Delta). \tag{13}$$

where K_p and K_d are positive constants, and $\Delta, \tau > 0$ are time delays.

Assuming that the sway angle is small, we can approximate $\sin(\theta) \approx \theta$ and we obtain a switched linear stochastic system

$$J\ddot{\theta} = mgh\theta + \sigma\zeta(t) \quad \text{for} \quad |\theta(t - \tau)| \leq \theta_0, \tag{14}$$

when there is no control applied to the system, and

$$J\ddot{\theta} = mgh\theta + T + \sigma\zeta(t) \quad \text{for} \quad |\theta(t - \tau)| > \theta_0. \tag{15}$$

when the PD controller is applied to it.

The phase space of the system is represented by $\theta(t)$ and $\dot{\theta}(t)$ which are the position and velocity components, respectively. The switchings occur after the delayed switching time τ takes place after passing the boundary of the dead zone. The system evolves according to the differential equation (14) when there is no control applied to the system, and according to the differential equation (15) when the PD control is applied to the system. The presence of the switching function implies that, depending on the value of the random variable $\theta(t - \tau)$, the system is either governed by a stochastic differential equation, or a stochastic delay differential equation. We switch between these two systems when the random variable $\theta(t - \tau)$ is greater or smaller than the threshold value θ_0.

We approach the modelling of human balancing by using switched control system with the noise term $\sigma\zeta(t)$. The dynamics of the deterministic system (14) and (15) was investigated in (Kowalczyk et al., 2011). Numerical simulations were performed with a fixed step size of $0.001s$ for the duration of $160s$. We set $m = 66$ kg, $h = 0.87$ m, $g = 9.81 m/s^2$, $J = 66$ kgm^2, time delays $\Delta = \tau = 0.15s$, the control coefficients $K_p = 720$ Nm/rad and $K_D = 300$ Nms/rad, which are the values used in (Kowalczyk et al., 2011). We assume that the width of the dead zone is equal to $|\theta| = 0.02$rad, which is approximately one degree. The data corresponding to the first $120s$ were discarded as describing transient dynamics, while the following $40s$ were recorded and used for the analysis. In the next subsections, we will analyze signals generated from our switched model of human balance control by using the designed algorithm. We perform numerical integration of our switched models with noise using an Euler's algorithm described in the appendix. For consistency, we also use a first order Euler's scheme for numerical integration in the absence of noise.

3.2. Case 1: Non-delayed switched system without noise ($\sigma = 0$, $\tau = 0$)

In this section, we investigate the effect of time delay in the switching function on the dynamics of the switched system. Thus, firstly, a human balance control model with time delay only in torque T will be investigated. By modifying equations (11) and (12) and assuming that the sway angle is small, we can approximate $\sin(\theta) \approx \theta$, and then we can obtain a switched linear system without time delay in the switching function in the form

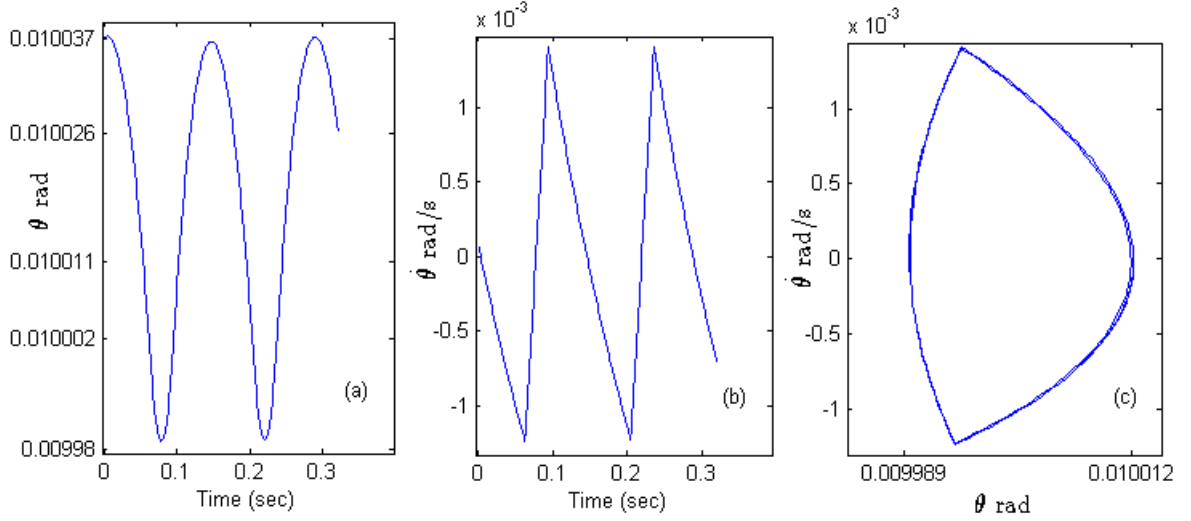$$J\ddot{\theta} = mgh\theta \quad \text{for} \quad |\theta(t)| \leq \theta_0, \tag{16}$$

10

Fig. 1: (a) Time series data of the position component of the switched system (16) and (17). (b) The velocity component. (c) Phase plot of the system.

$$J\ddot{\theta} = mgh\theta - K_p(t - \Delta)\theta - K_d(t - \Delta)\dot{\theta} \quad \text{for} \quad |\theta(t)| > \theta_0. \tag{17}$$

Fig. 1 shows the angular position component θ, the angular velocity component $\dot{\theta}$, and the phase plot of the time series data produced by the modified switched model system. In our analysis we use the angular position data corresponding to the first two limit cycle attractors. The period of each limit cycle will be approximately 0.165 seconds.

We have applied the proposed algorithm to analyze the produced time series data. The algorithm accurately locates the change points in the data where the trajectory crosses the dead zone of the system. As shown in Fig. 2 these discontinuities occur at $t = 0.065s$, and $t = 0.095s$ for the limit cycle in the first period, and at $t = 0.207s$, and $t = 0.237s$ for the limit cycle in the second period. Note that the limit cycle attractor is built from two smooth trajectory segments and there are two points on the limit cycle where the trajectory looses it smoothness as a direct result of switchings between two regions where the variable $\theta(t)$ is greater or smaller than the threshold value θ_0. Therefore, in one time period, the discontinuity occurs at two times in the time series data. This suggests that the computed instantaneous frequency is able to capture the discontinuities produced by the non-delayed switched control system without noise.

3.3. Case 2: Non-delayed switched system with additive noise ($\sigma \neq 0$, $\tau = 0$)

In order to further investigate the capability of the developed method to detect the discontinuities in a switched stochastic system without time delay, we modify our model system to include Gaussian
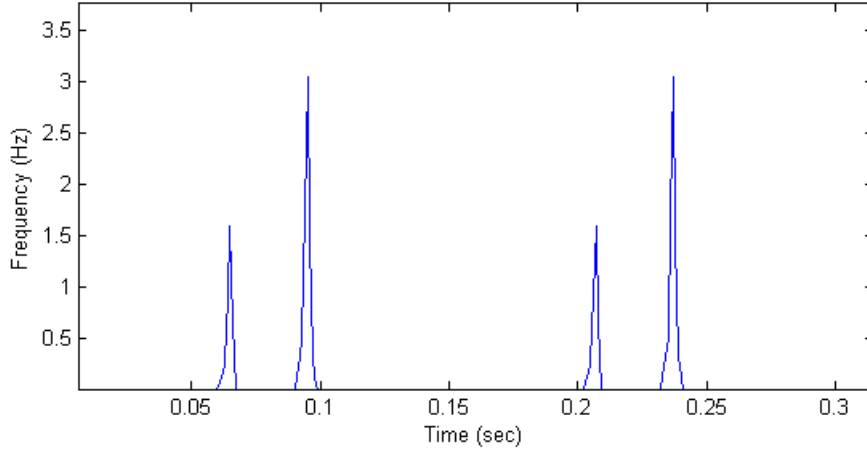
Fig. 2: Time-frequency representation of the switched stochastic system 16) and (17).

noise term according to the following stochastic differential equations

$$J\ddot{\theta} = mgh\theta + \sigma\zeta(t) \quad \text{for} \quad |\theta(t)| \leq \theta_0, \tag{18}$$

$$J\ddot{\theta} = mgh\theta - K_p\theta(t - \Delta) - K_d\dot{\theta}(t - \Delta) + \sigma\zeta(t) \quad \text{for} \quad |\theta(t)| > \theta_0. \tag{19}$$

Fig. 3 shows the angular position component θ, the angular velocity component $\dot{\theta}$, and the phase plot of the system. In this case, adding white noise to this system will result in sample path (trajectory) following the underlying limit cycle attractor as depicted in Fig. 3(c). We used a time window of 0.32 seconds, which is approximately the length of time at tow periods of evolution of the corresponding limit cycle attractor.

In this case, the high frequency noise will disturb the detection process, therefore, an efficient filtering operation is essential to decompose the data to monocomponent functions. The stationary discrete wavelet transform was applied to decompose the data into seven levels as shown in Fig. 4. The wavelet decomposition technique brings out a high resolution data which are the details coefficients, while at the same time it extracts the remaining data as approximation coefficients. Here, we are interested in examining the details coefficients. By performing the energy entropy based method, and exploring all the levels, it was found that the first five levels are irrelevant because they consist mostly of the high frequency noise. The frequency analysis method only applies to the two remaining levels where we can isolate the presence of harmonics, thereby confirming the presence of the underlying limit cycle attractors. Hence, levels six and seven of the details monocomponents were reconstructed for further analysis, while the other levels were considered irrelevant because they consist mostly of the high frequency noise.

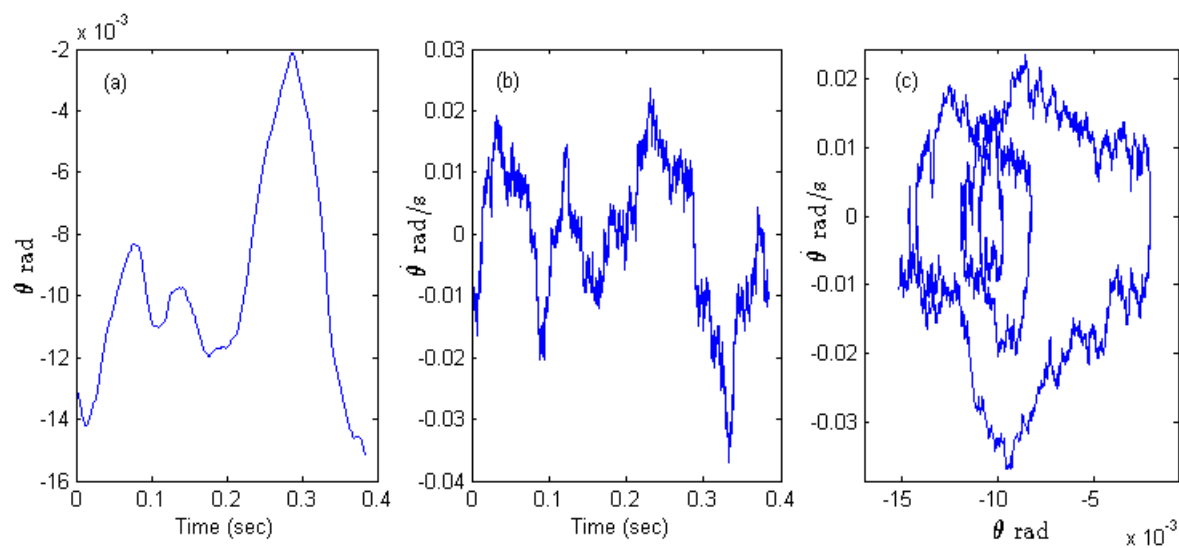The algorithm starts the normalization process by calculating Hilbert's envelop to reconstructed

12

Fig. 3: (a) Time series data of the position component of the stochastic system (18) and (19). (b) The velocity component. (c) Phase plot of the system.
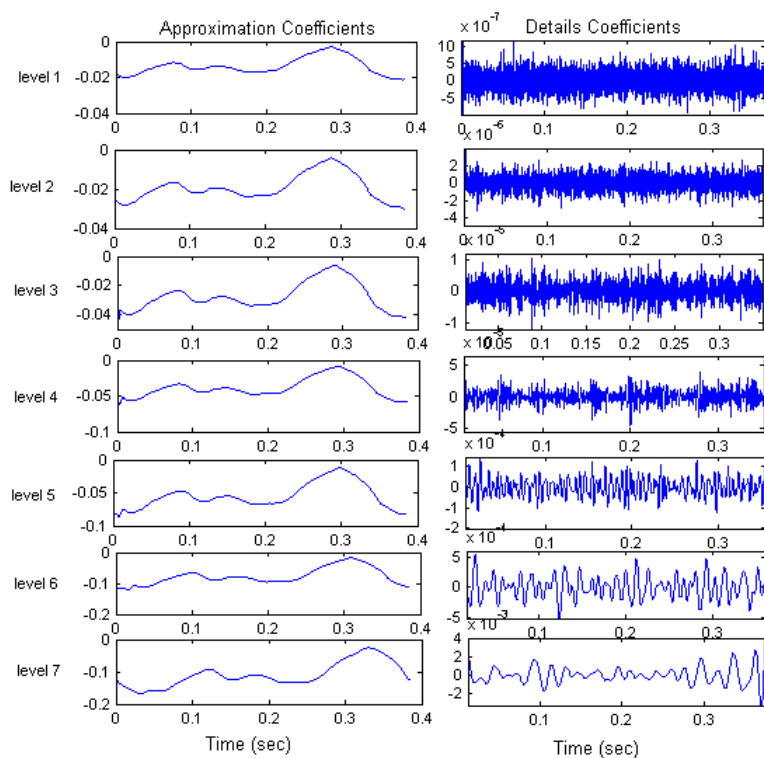

Fig. 4: Wavelet approximation coefficients (left columns), and wavelet details coefficients (right column).
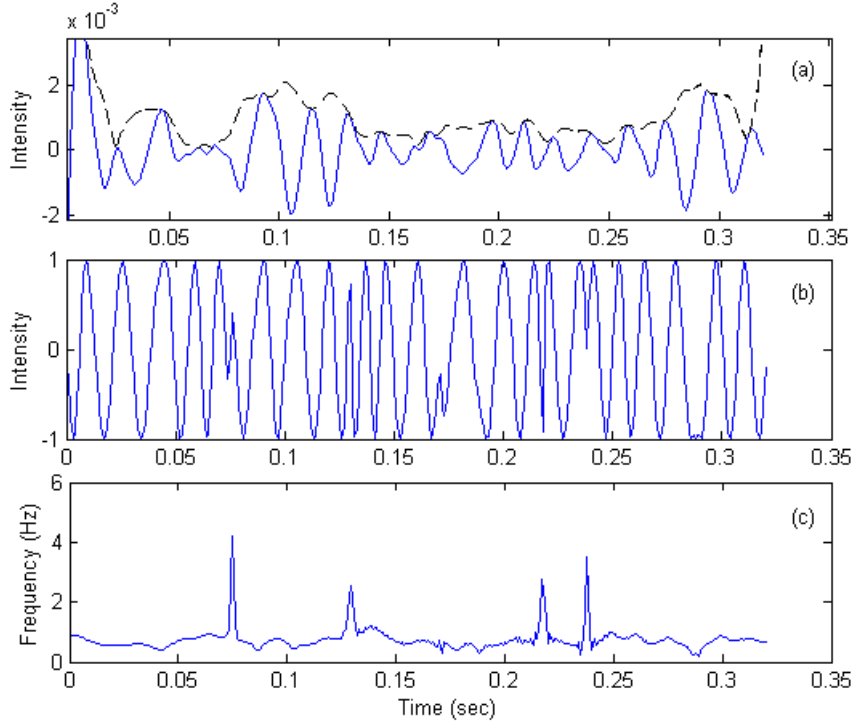
13

Fig. 5: (a) The reconstructed data (solid line), with Hilbert's envelop (dashed line). (b) Normalized data by Hilbert transform. (c) The computed instantaneous frequencies of the switched system (18) and (19).

data from the wavelet details coefficients. Fig. 5(a) shows the time series data with the calculated Hilbert's envelop. Fig. 5(b) presents the produced signal after the normalization scheme where all of the values of the signal are less than or equal to unity. This normalized carrier enables us to provide a ready and sharper local energy based measure of any abrupt changes. The instantaneous frequency of the data can then be computed by applying Hilbert transform. This approach will enable us to get an exact instantaneous frequency as a derivative of the phase function. Fig. 5(c) shows the time-frequency presentation of the time series data generated by our stochastic model system. Four major instantaneous frequency peaks can be detected within this time period which correspond to the discrete jumps that are present in the signal derivatives. These discontinuities occur at $t = 0.075s$, $t = 0.129s$, $t = 0.217s$ and $t = 0.238s$ for the time window 0.32 seconds.

As it can be seen in Fig. 5(c), the discontinuities occur at each limit cycle period as in the previous case. However, there is a slight shift in the identified peaks. We believe this is because of the influence of noise on the instances when switchings occur.

3.4. Case 3: Time-delayed switched system without noise ($\sigma = 0$, $\tau \neq 0$)

Similarly, we analyze the time series data produced by our switched model system (14) and (15) without the noise term. Fig. 6 shows the angular position component θ, the angular velocity component $\dot{\theta}$, and the phase plot of the system. According to equation (14), the PD control is not
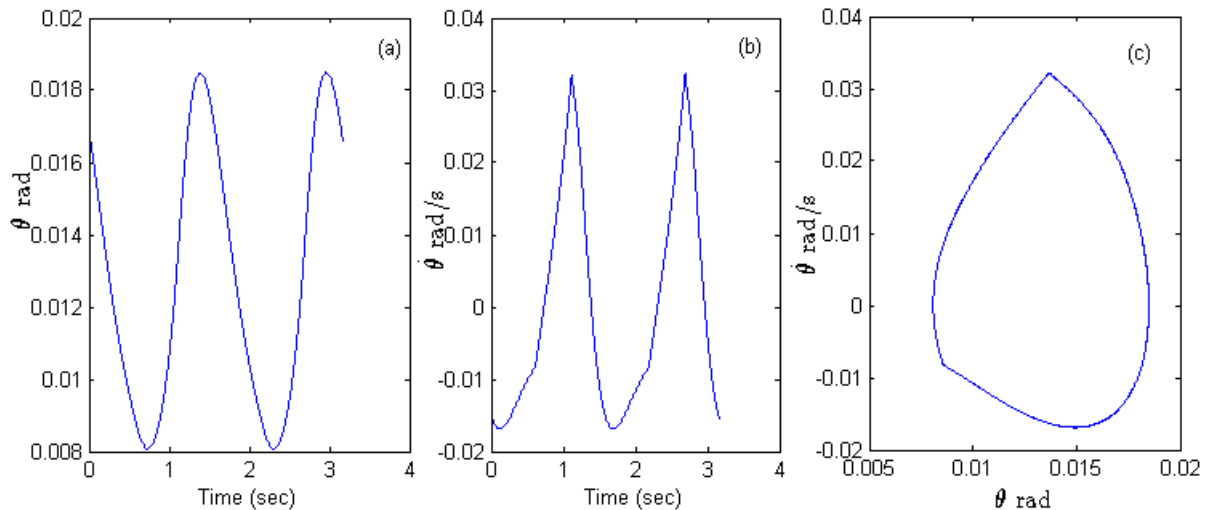
Fig. 6: (a) Time series data of the position component of the switched system (14) and (15) without noise. (b) The velocity component. (c) Phase plot of the switched system.

active so the switched system is not controllable, and all the trajectories diverge to $\pm\infty$. Once the delayed control signal $\theta(t-\tau)$ reaches the value of $\pm\theta_0$, that is the boundary of the dead-zone, the system switches on the PD control, and the evolution follows according to equation (15). As a result of applying the PD control, the system trajectory will move back within the dead-zone region, and will finally converge to a limit cycle attractor as shown in the phase space plot in Fig. 6(c). Therefore, stable periodic motion is found. Due to the system's symmetry, for any given parameter values, there are two limit cycle attractors present in the system. For the purpose of our analysis, we use the angular position data corresponding to the first two limit cycle attractors. In this case, the period of each limit cycle is approximately 1.656 seconds. Fig. 7 shows the results of applying the algorithm to the time series data produced by the switched system. The time-frequency representation has been used to illustrate the detection of discontinuous nonlinearities at different time locations in the time series data. As we can see in Fig. 7, the discontinuities occur at $t = 0.631s$ and $t = 1.116s$ for the limit cycle in the first period, and at $t = 2.188s$ and $t = 2.69s$ for the limit cycle in the second period. The algorithm accurately locates the change points in the time series data. This suggest that the computed instantaneous frequency is able to capture the discontinuity produced by the switched control system without additive noise.

3.5. Case 4: Time-delayed switched system with additive noise ($\sigma \neq 0$, $\tau \neq 0$)

In order to investigate the influence of the additive white noise, we have analyzed the time series data produced by the switched stochastic control system (14) and (15). Adding white noise to the system may cause the switching of the evolution between neighbourhoods of the two asymmetric
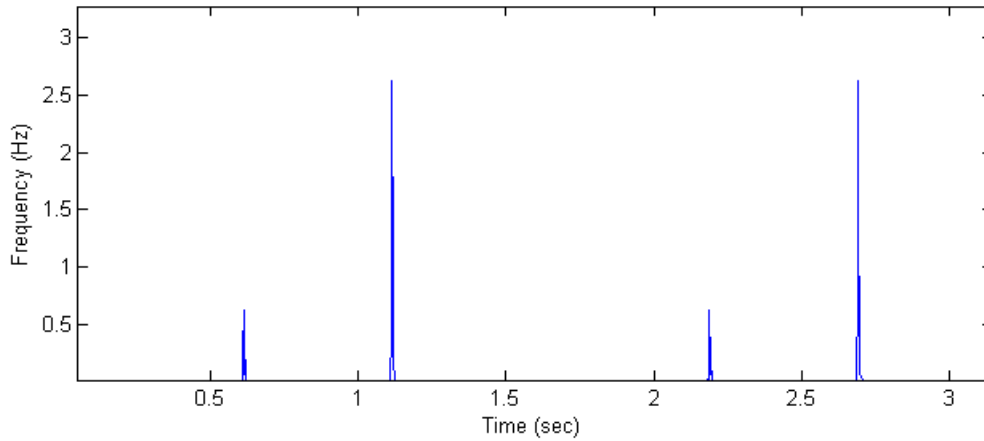
15

Fig. 7: Time-frequency representation of the switched system (14) and (15) without noise.

limit cycles present in the switched system in the absence of noise. An example of a stochastic run is shown in Fig. 8.

As shown in Fig. 9, the output was a series of peaks, each of which occurred when the system switches between two different modes. Each peak seen in the analyzed results corresponds to the event when the system trajectory crosses the line of the dead-zone region. Similarly as in the case of the non-delayed system (18) and (19), there is a slight shift in the identified peaks as a result of the influence of noise on the instances when switchings occur.

3.6. Case 5: Analysis of posturographic data

In this section, we will present the results of analyzing experimentally obtained data sets of human sway during quiet stance. We consider the time series data of human subjects standing quietly with eyes closed or open. The data were collected at the IRM (Institute of Research into Human Movement) laboratory at Manchester Metropolitan University. Eight people, with no balance disorders, participated in the study. Each subject was standing quietly with eyes open for the duration of 240s. Horizontal and vertical ground reaction forces were measured using a force plate with four strain gauge sensors (OR6-7; AMTI, Watertown, MA). The position of the center of pressure of the forward-backward and side-to-side body sway was calculated from the ground reaction forces. The time series data were recorded and sampled at 1 kHz. The experiment was then repeated with eyes closed. For the purposes of analysis, we expressed the force signal as angular position and velocity data. The signal was then filtered using lowpass butterworth filter with the cut off frequency of 4Hz. Fig. 10 shows the time series and phase plot of one of the collected experimental posturographic data sets.

The algorithm procedure was performed in order to analyze the time series data. We used a time window of 3.2 seconds which is approximately similar to the sample path that follows the first
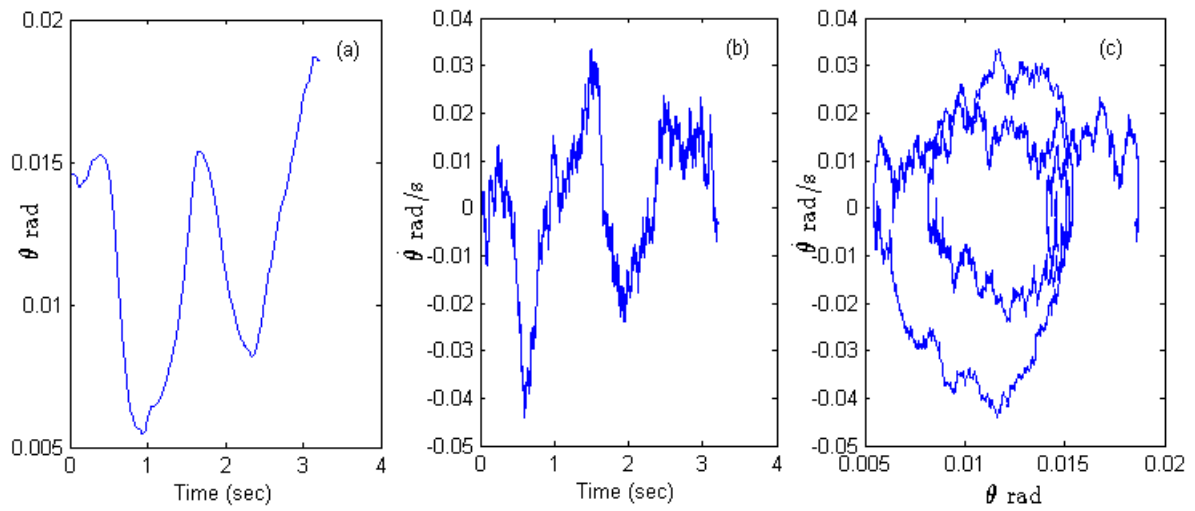
Fig. 8: The trajectory of the position component of the switched system with added white noise. (b) The velocity component. (c) Phase plot of the switched system.
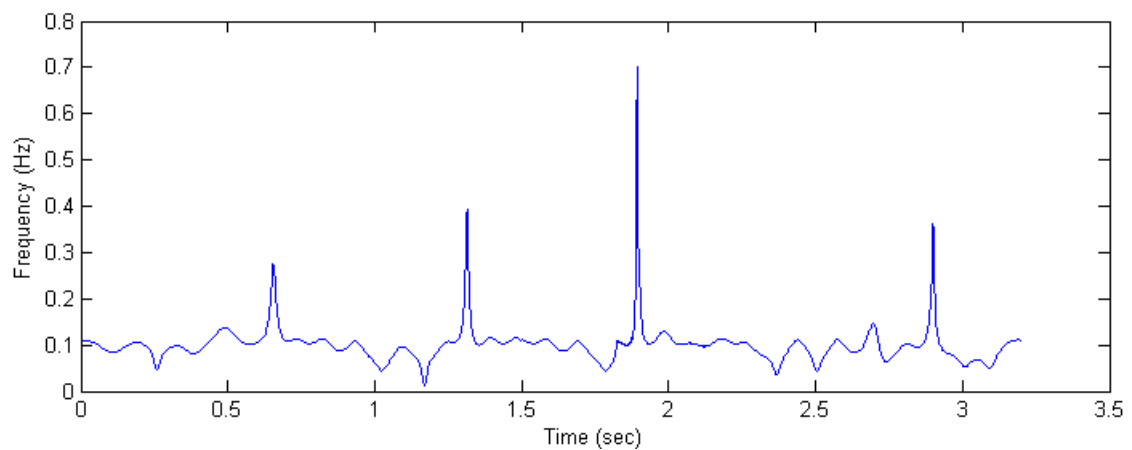

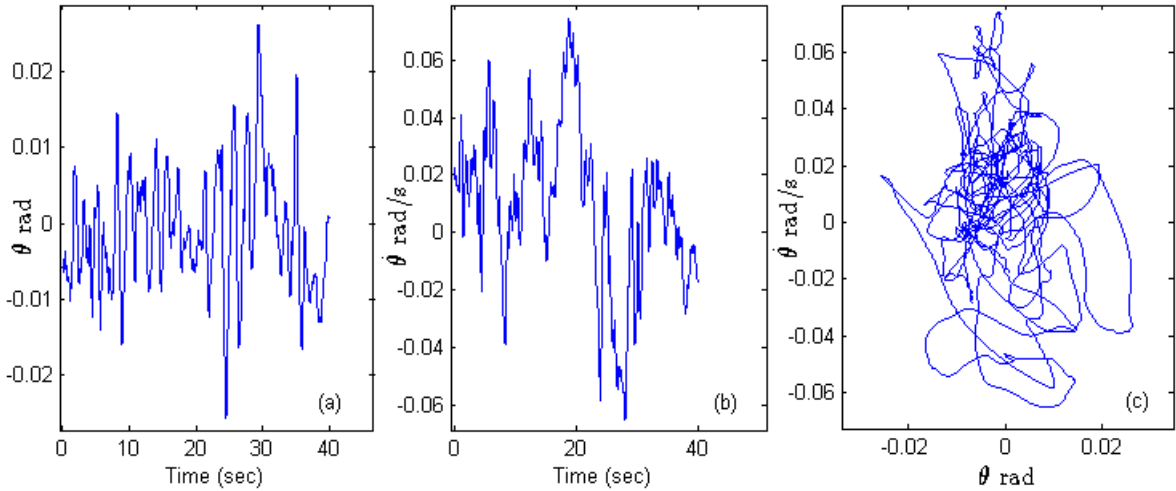Fig. 9: Time-frequency representation of the switched stochastic system (14) and (15).

17

Fig. 10: (a) Time series data of the angular position of the experimental posturographic data. (b) The angular velocity. (c) Phase plot of the data.

two underlying limit cycle attractors produced by the switched stochastic system (14) and (15). We first decompose the data by using the discrete wavelet transform process to isolate the low and high frequency components. This step produces two complementary components for further analysis-details coefficients and approximation coefficients, and the original signal is broken down into many lower resolution components. The first few levels of the details coefficients are small and consist mainly of a high frequency noise. These levels are therefore discarded. Only coefficients that convey most of the information of the signal are considered for further analysis. These components are reconstructed by using the inversion process. Fig. 11 shows the computed instantaneous frequencies of the reconstructed data. The algorithm identifies different peaks corresponding to abrupt changes in the signal. These spikes indicate features such as a jump, or discontinuity in the time series data. It can be noted that simulated and experimental data have similar spectral properties during each time window.

3.7. Algorithm Performance Evaluation

The results suggest that the algorithm works well in different cases and is capable of locating the discontinuities for all the model systems in the present study in a reliable manner. The obtained results confirm the ability of the developed algorithm to handle sharp changes in the characteristic properties of the signal generated by a stochastic process.

For quantitative purposes, we apply the designed algorithm to the time series data produced by the model system (18) and (19) for a time window of 0.192 seconds, which is the time required to make one revolution around the underlying limit cycle attractor. We compute the Fourier power
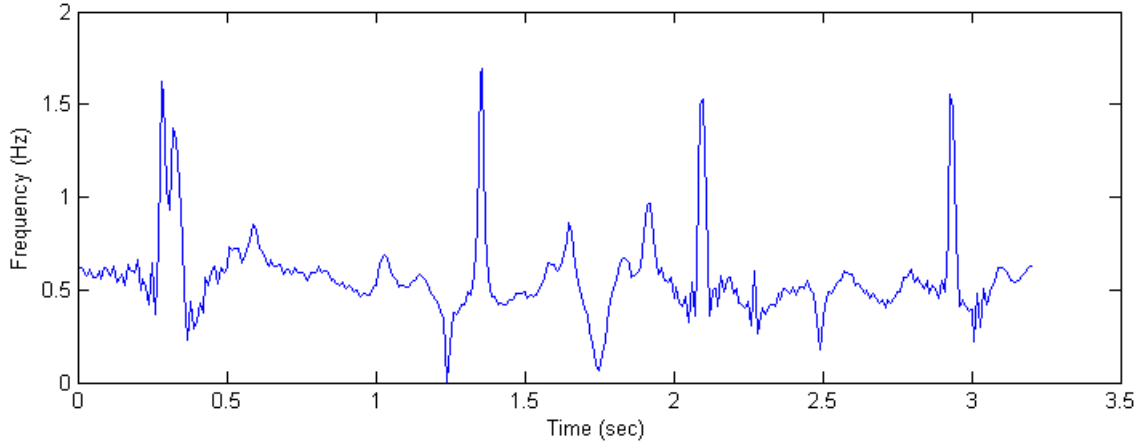
Fig. 11: The instantaneous frequencies of experimental data within a time window of 3.2 seconds.

spectrum for all the signals at each decomposition level. The total power present in harmonic frequencies is then determined. The algorithm identifies two peaks by analysing the sixth and seventh decomposition levels. The power contribution from the identified peaks is calculated by dividing the power summation of the captured peaks by the total power present in all the decomposition levels. It is found that the amount of power in the identified peaks is 14.2 % of the power in the original signal. Thus, the algorithm is able to capture the discontinuities having a relatively low power content.

The previous simulated results are for single realizations only. Using Monte Carlo simulations, we have examined the probability of detection performance of the algorithm for all the model systems (case 1 to 4). Here, we examine the effect of varying the intensity σ of each realization of the white Gaussian noise process by averaging MC=100 Monte Carlo simulations. The different intensity of white Gaussian noise denotes different levels of noisy environment. Fig. 12 shows the probability of detection as a function of the noise intensity σ. The results show that, as the noise intensity σ is increases, the probability of detection for the algorithm decreases.

Furthermore, when we applied our algorithm to posturographic data of human balance control during quiet standing, we observed approximately one to two peaks per second in the time-frequency representation, as it is shown in Fig. 9. This observation is consistent with the hypothesis (Loram et al., 2009; Navas and Stark, 1968) that control via serial ballistic actions, at a rate of two per second, is generic to human motor control. Moreover, the spikes which we found in the time-frequency plot of the analyzed experimental data were qualitatively similar to those found in our switched model systems.
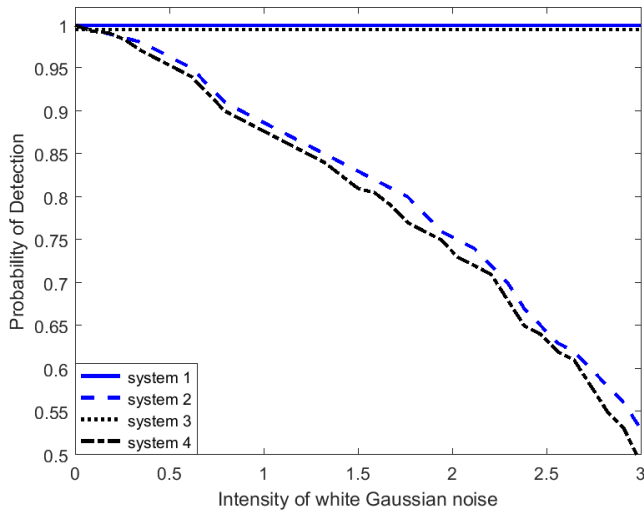
Fig. 12: The probability of detection for the switched model systems (case 1 to 4) varies with the intensity of white Gaussian noise.

4. Conclusions

In this work, we propose a method that uses wavelets and frequency analysis for the detection of discontinuity in switched control systems with noise. Simulation results, based on analyzing time series data produced by four different switched feedback control systems with (and without) noise and time delay, which are models used in the context of human balance control during quiet standing, demonstrate that discontinuous nonlinearities manifest themselves as spikes in the time-frequency plane.

A review of observations from the neuro-motor control literature (Gawthorp et al., 2011; Loram et al., 2011, 2009) reveals that there is evidence of intermittent control in human movement. For instance, Loram et al. (Loram et al., 2011) showed that, when using a joystick to control an unstable load that falls over, like a person fainting, the control using intermittent gentle hand taps with the frequency of 1-2 taps per second, that one can make without mutual interference between movements is an optimal control strategy. We applied the proposed method to posturographic time series data and found the presence of spikes in the time-frequency plane with the average frequency of spikes of 4 per 3.2 seconds in switched models (18) and (19). Thus, it is the switched model with time delay in the control and switching function which captures better the presence of discontinuities in the posturographic data. Our results give evidence for the presence of intermittent control in human neuro-muscular control system. Future work is aimed at continuing to test the designed algorithm under a variety of conditions in order to distinguish between different types of discontinuities, or strong nonlinearities, that can be captured by means of the developed algorithm.

20

Acknowledgment

Appendix

Switched system (14)-(15) is a stochastic delay differential equation. It has been shown in (Baker and Buckwar, 2000) that stochastic delay differential equations

$$\dot{x} = f(x(t), x(t - \tau)) + \sigma\zeta(t), \tag{20}$$

where τ is the time delay, ζ is Gaussian white noise with intensity σ, can be approximated by

$$x_{n+1} = x_n + f(x_n, x_{n-k})h + \sigma W_n\sqrt{h}, \tag{21}$$

for h sufficiently small; τ is the time delay, h is the step size, $k = \tau/h$ and W_n is the standard Wiener process. The standard Wiener process is approximated numerically at each step t_n by a function which generates pseudo-random numbers with expected value $\mu = 0$ and standard deviation $\sigma = 1$. The same numerical scheme may be used when there is no delay present in the system. If we integrate the system with the time delay in the switching function, we switch between different systems at some step n when $(\theta(t_n - t_{n-k}) - \theta_0)(\theta(t_{n-1} - t_{n-1-k}) - \theta_0) < 0$ (the value $\theta_0 > 0$ determines the width of the dead-zone). When there is no time delay in the switching decision function the switching condition at step n reduces to $(\theta(t_n) - \theta_0)(\theta(t_{n-1}) - \theta_0) < 0$.

References

Antoniadis, A. and Gijbels, I. (2002). Detecting abrupt changes by wavelet methods. *Journal of Nonparametric Statistics*, 14:7–29.

Babji, S., Gorai, P., and Tangirala, A. (2009). Detection and quantification of control valve nonlinearities using hilbert-huang transform. *Advances in Adaptive Data Analysis*, 1:425–446.

Baker, C. and Buckwar, E. (2000). Numerical analysis of explicit one-step methods for stochastic delay differential equations. *London Mathematical Society Journal of Computational Mathematics*, 3:315–335.

Boashash, B. (1992). Estimating and interpreting the instantaneous frequency of a signal. *Proceedings of the IEEE*, 80:520–538.

Bottaro, A., Yasutake, Y., Nomura, T., Casadio, M., and Morasso, P. (2008). Bounded stability of the quiet standing posture:an intermittent control model. *Human Movement Science*, 27:47317495.

Craik, K. (1947). Theory of the human operator in control systems: I. the operator as an engineering system. *British Journal of Psychology*, Gen Sect 38:56–61.

Daubechies, I. (1992). Ten lectures on wavelets. *CBMS-NSF Series in Applied Mathmatics.SIAM, Philadelphia*, 61.

Gammaitoni, L. (1995). Stochastic resonance and the dithering effect in threshold physical systems. *Phys. Rev. E*, 52:4691–4698.

Gawthorp, P., Loram, I., Lakie, M., and Gollee, H. (2011). Intermittent control: a computational theory of human control. *Biological Cybernetics*, 104:31–51.

Huang, N., Wu, Z., Long, S., Arnold, K., Chen, X., and Blank, K. (2009). On instantaneous frequency. *Advances in Adaptive Data Analysis*, 1:177–299.

Inoue, Y. and Sakaguchi, Y. (2015). A wavelet-based method for extracting intermittent discontinuities observed in human motor behavior. *Neural Networks*, 62:91–101.

Jeka, J., Kiemel, T., Creath, R., Horak, F., and Peterka, R. (2004). Controlling human upright posture: Velocity information is more accurate than position or acceleration. *Journal of Neurophysiology*, 92:2368 – 2379.

Jeka, J. J., Oie, K. S., and Kiemel, T. (2000). Multisensory information for human postural control: integrating touch and vision. *Experimental Brain Research*, 134:107–125.

Kiemel, T., Oie, K. S., and Jeka, J. J. (2002). Multisensory fusion and the stochastic structure of postural sway. *Biological Cybernetics*, 87:262–277.

Killick, R. and Eckley, I. (2013). A wavelet-based approch for detecting changes in second order structure within nonsatationary time series. *Electronic Journal of Statistics*, 7:1167–1183.

Kowalczyk, P., Glendinning, P., Brown, M., Medrano-Cerda, G., Dallali, H., and Shapiro, J. (2011). Modelling human balance using switched systems with linear feedback control. *Journal of the Royal Society Interface*, 9:234–245.

Liu, Z., Li, H. X., and Zhang, Y. (2008). A probabilistic wavelet system for stochastic and incomplete data-based modeling. *IEEE Trans. on System Man and Cybernetics Part B*, 38(2):310–319.

Liu, Z., Zhang, Y., and Wang, Y. (2007). A type-2 fuzzy switching control system for biped robots. *IEEE Trans. on System Man and Cybernetics Part C*, 37(6):1202–1213.

Loram, I., Gollee, H., Lakie, M., and Gawthrop, P. (2011). Human control of an inverted pendulum: Is continuous control necessary? is intermittent control effective?is intermittent control physiological? *The Journal of Physiology*, 589(2):307–324.

Loram, I., Lakie, M., and Gawthorp, P. J. (2009). Visual control of stable and unstable loads: what is the feedback delayand extent of linear time-invariant control ? *Journal of Physiology*, 587:1342–1365.

Marple, S. (1999). Computing the discrete-time analytic signal via fft. *IEEE Transactions on Signal Processing*, 47:52600–2603.

Navas, F. and Stark, L. (1968). Sampling or intermittency in hand control system dynamics. *Biophys J*, 8:252–302.

Richman, J. S. and Moorman, J. R. (2000). Physiological time-series analysis using approximate entropy and sample entropy. *Am J Physiol Heart Circ Physiol*, 278:H2039–H2049.

Strang, G. and Nguyen, T. (1997). *Wavelets and filter banks*. Wellesley Cambridge Press.

Theron, J. and Aldrich, C. (2004). identification of nonlinearities in dynamic process systems. *Journal of the South African Institute of Mining and Metallurgy*, 104:191C200.

Thornhill, N. and Horch, A. (2007). Advances and new directions in plant-wide disturbance detection and diagnosis. *Cont. Eng. Pract.*, 15:1196–1206.

Winter, D. A., Patla, A. E., Riedtyk, A. E., and Ishac, M. (2001). Ankle muscle stiffness in the control of balance during quiet standing. *Journal of Neurophysiology*, 85:2630–2633.